ARTICLE

doi:10.1038/nature18634

Human commensals producing a novel antibiotic impair pathogen colonization

Alexander Zipperer[1,2]*, Martin C. Konnerth[3]*, Claudia Laux[1,2], Anne Berscheid[4], Daniela Janek[1,2]†, Christopher Weidenmaier[2,5], Marc Burian[6], Nadine A. Schilling[3,7], Christoph Slavetinsky[1,2], Matthias Marschal[5], Matthias Willmann[2,5], Hubert Kalbacher[7], Birgit Schittek[6], Heike Brötz-Oesterhelt[2,4], Stephanie Grond[3], Andreas Peschel[1,2] & Bernhard Krismer[1,2]

The vast majority of systemic bacterial infections are caused by facultative, often antibiotic-resistant, pathogens colonizing human body surfaces. Nasal carriage of *Staphylococcus aureus* predisposes to invasive infection, but the mechanisms that permit or interfere with pathogen colonization are largely unknown. Whereas soil microbes are known to compete by production of antibiotics, such processes have rarely been reported for human microbiota. We show that nasal *Staphylococcus lugdunensis* strains produce lugdunin, a novel thiazolidine-containing cyclic peptide antibiotic that prohibits colonization by *S. aureus*, and a rare example of a non-ribosomally synthesized bioactive compound from human-associated bacteria. Lugdunin is bactericidal against major pathogens, effective in animal models, and not prone to causing development of resistance in *S. aureus*. Notably, human nasal colonization by *S. lugdunensis* was associated with a significantly reduced *S. aureus* carriage rate, suggesting that lugdunin or lugdunin-producing commensal bacteria could be valuable for preventing staphylococcal infections. Moreover, human microbiota should be considered as a source for new antibiotics.

Infections caused by highly antibiotic-resistant bacteria have greatly increased in recent years and represent a major cause of morbidity and mortality worldwide, including in developed countries[1,2]. Multidrug resistant organisms (MDRO), such as methicillin-resistant *S. aureus*[3], vancomycin-resistant enterococci[4], and third-generation cephalosporin-resistant Gram-negative bacteria[5], are expected to become more frequent causes of death than cancer in the coming decades[6]. Despite the urgent need for new antibiotics that are effective against resistant bacteria, very few compounds are in development, the majority of which are congeners of currently used antibiotic classes[7,8]. Nevertheless, innovative approaches for cultivation of yet uncultured potential antibiotic producers or activation of silent biosynthetic gene clusters have recently led to the discovery of entirely new antimicrobial compounds with useful properties[9–12]. Moreover, new compound sources, such as the large inventory of antimicrobial host defence peptides from higher organisms, open new avenues for the development of new anti-infectives[13,14]. As the available antibiotics lose their efficacy, it is important to limit the ongoing spread of resistant bacteria[15]. Unfortunately, most of the major MDROs are increasingly disseminating in the community and cannot be effectively targeted by standard infection-control measures[2]. The strong antibiotic selection pressure in humans and in farm animals and the increasing fitness of methicillin-resistant *S. aureus*, vancomycin-resistant enterococci, and third-generation cephalosporin-resistant Gram-negative bacteria in competition with commensals leads to the symptomless and usually unrecognized presence of MDRO in the microbiota of many humans[16–18]. Notably, the vast majority of systemic bacterial infections are caused by endogenous pathogens from human microbiota, and MDRO-colonized individuals are exposed to a substantially higher risk of invasive infections, that are difficult to treat, when they undergo surgery or immunosuppression, or suffer from trauma[1,19,20]. *S. aureus* is found in the anterior nares of approximately 30% of the human population. Eradication by the antibiotic mupirocin strongly reduces predisposition to invasive infection[19]. However, mupirocin has to be applied repeatedly over five days, requiring strict compliance and costly extension of patient hospitalization; in addition, rates of mupirocin resistance are steadily increasing[21]. Moreover, current decolonization strategies targeting MDRO at other body surfaces, such as the intestine, depend on broad-spectrum antibiotics and are highly controversial[22]. Thus, there is not only an urgent need for new therapeutic antibiotics but also for new effective MDRO decolonization strategies.

Although many ongoing research efforts address major virulence and resistance mechanisms, the processes governing bacterial fitness, competition, and dissemination in microbiota remain poorly understood. Recent studies have shown how diverse and dynamic human microbiota are, especially those of the environment-exposed microbiota of the skin[23] and upper airways[24]. These ecological niches are particularly poor in nutrients[25], suggesting that colonizing bacteria are probably in strong competition and may use a variety of strategies to overcome competitors[25,26]. Bacteria from human microbiota have occasionally been found to produce bacteriocins, antimicrobial substances acting against closely related bacteria[27,28]. Genes related to antibiotic biosynthesis have been identified in human metagenomes[29] leading to the discovery of lactocillin, a ribosomally synthesized thiopeptide antibiotic produced by a human vaginal commensal[30]. However, the potential roles of such complex bioactive compounds in shaping human microbiota are still unknown.

Antimicrobial activity of a nasal commensal

A previously described collection of nasal *Staphylococcus* isolates[25] was screened for antimicrobial activity against *S. aureus*. Whereas most

[1]Interfaculty Institute of Microbiology and Infection Medicine, Infection Biology, University of Tübingen, 72076 Tübingen, Germany. [2]German Centre for Infection Research (DZIF), Partner Site Tübingen, 72076 Tübingen, Germany. [3]Institute of Organic Chemistry, University of Tübingen, 72076 Tübingen, Germany. [4]Interfaculty Institute of Microbiology and Infection Medicine, Microbial Bioactive Compounds, University of Tübingen, 72076 Tübingen, Germany. [5]Interfaculty Institute of Microbiology and Infection Medicine, Medical Microbiology, University of Tübingen, 72076 Tübingen, Germany. [6]Department of Dermatology, Division of Dermatooncology, University of Tübingen, 72076 Tübingen, Germany. [7]Interfaculty Institute of Biochemistry, University of Tübingen, 72076 Tübingen, Germany. †Present address: Boehringer Ingelheim, 88400 Biberach, Germany.
*These authors contributed equally to this work.

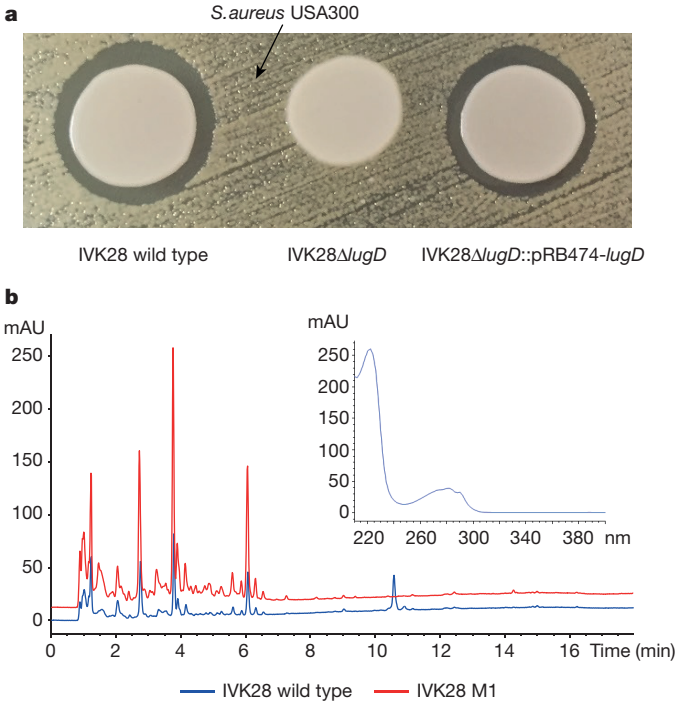

Figure 1 | Lugdunin production by wild-type *S. lugdunensis* and isogenic mutants. a, Bioactivity assay with the *S. lugdunensis* IVK28 wild type, the Δ*lugD* mutant and the complemented mutant against *S. aureus* USA300. Basic medium plates were inoculated with a lawn of *S. aureus* USA300. *S. lugdunensis* IVK28 cells from overnight cultures of wild type, the lugdunin-deficient deletion mutant Δ*lugD* and complemented mutant Δ*lugD*::pRB474-*lugD* were spotted onto the plates. **b**, HPLC-UV-chromatogram shows comparison of *S. lugdunensis* IVK28 wild type and the lugdunin-deficient transposon mutant M1. Cell extracts of the IVK28 wild type (blue) and the transposon mutant M1 (red) were compared by reversed-phase HPLC-UV. The inlay depicts the absorption spectrum of lugdunin with the prominent absorption at 280 nm, indicating the presence of tryptophan. Absorbance was measured in milli absorption units (mAU).

isolates did not affect *S. aureus*, the strain *S. lugdunensis* IVK28 was found to have a particularly strong capacity to prevent the growth of *S. aureus* (Fig. 1a). IVK28 produced an antibacterial substance only under iron-limiting conditions and only on solid agar surfaces, not in liquid culture.

Transposon mutagenesis of IVK28 led to isolation of mutant M1, which did not inhibit *S. aureus*. Analysis of the transposon insertion site revealed the disruption of an uncharacterized gene encoding a putative non-ribosomal peptide synthetase (NRPS; position 860375/76 of SLUG_RS03940 in the annotated genome sequence of *S. lugdunensis* N920143 ref. 31; accession number, NC_017353.1). This gene is encoded in an operon of approximately 30 kbp with several other NRPS and antibiotic biosynthesis-related genes (Fig. 2a and Extended Data Fig. 1a), suggesting that the inhibitory molecule of IVK28 may be a complex, non-ribosomally synthesized peptide compound. The NRPS operon was found in all *S. lugdunensis* genomes in the databases, and it was identified by PCR in each of the *S. lugdunensis* strains from our strain collection, indicating that it is characteristic of the species, rather than a strain-specific feature. Nevertheless, the GC-content of the operon of 26.9% is clearly distinct from that of the whole genome (33.8%) indicating that the gene cluster may have been transferred to *S. lugdunensis* by horizontal gene transfer from another bacterial species. The operon consists of four NRPS genes (named *lugA, B, C, D*) encoding adenylation domains for five amino acids (Fig. 2b). The *lug* operon further includes all genes whose products are required for the synthesis and transport of a non-ribosomally synthesized peptide compound (Extended Data Fig. 1a). Gene clusters for secondary metabolite production are frequently found in streptomycetes and other soil bacteria but are rare in human-associated bacteria[29]. The *lug* operon was exclusively found in *S. lugdunensis* and encodes a unique combination of antibiotic biosynthesis enzymes, all with less than 35% identity to any other described enzyme, suggesting that it may be responsible for biosynthesis of a novel compound. To confirm that the *lug* operon is responsible for the antimicrobial activity of IVK28, the smallest NRPS gene, *lugD*, was deleted by gene replacement. The mutant Δ*lugD* showed no detectable antimicrobial activity, but the phenotype was restored by complementation with a plasmid-encoded copy of *lugD* (Fig. 1a).

Lugdunin, a novel peptide antibiotic

The antimicrobial activity of IVK28 was enriched by ethanol extraction of agar-grown cells. Reversed-phase high-pressure liquid chromatography (HPLC) coupled with ultraviolet (UV) and mass spectrometry revealed obvious differences between extracts from IVK28 wild-type and mutant M1 in only one signal (Fig. 1b). The molecular formula, $C_{40}H_{62}N_8O_6S$, deduced from electrospray ionization high-resolution mass spectrometry (Extended Data Fig. 2a, b; $[M+H]^+$ $C_{40}H_{63}N_8O_6S^+$, calculated 783.45858, found 783.45850, Δ0.1 parts per million (p.p.m.), relative molecular mass = 783.03) did not correspond to any known molecule. Spectral UV absorbance at 280 nm indicated the presence of a tryptophan moiety (Fig. 1b). As the compound was not produced in liquid culture, which impeded isolation of sufficient amounts for chemical characterization and biological profiling, expression of the biosynthetic genes was uncoupled from the native *lug* operon promoter and its regulation. This strategy has recently been successfully applied to other antimicrobial gene clusters[10,32,33]. The putative *tetR*-like regulator gene of the *lug* operon (*lugR*) was deleted, and the strong *xylAB* promoter was inserted upstream of the NRPS genes, along with the gene for its corresponding xylose-sensitive repressor XylR. Cultivation of the resulting strain *S. lugdunensis* IVK28-Xyl (Extended Data Fig. 1b) in liquid culture with xylose led to strong production of inhibitory activity, which could be purified by consecutive steps of 1-butanol extraction, gel filtration, and reversed-phase HPLC. The pure compound exhibited exactly the same mass as determined for the compound from the wild-type strain IVK28 and was named lugdunin.

Nuclear-magnetic resonance (NMR), electrospray ionization high-resolution mass spectrometry, and an advanced Marfey's analysis of lugdunin revealed a cyclic peptide (Fig. 2c, Extended Data Fig. 3a–e, and Extended Data Table 1) comprising an unusual thiazolidine heterocycle and five amino acids (D-valine, L-tryptophan, D-leucine, L-valine, and D-valine) (Fig. 2c). The thiazolidine building block occurs in certain linear NRPS products, such as watasemycins[34] and yersiniabactin[35], but is yet unreported in macrocyclic peptides (Extended Data Fig. 4). The lugdunin thiazolidine ring is probably formed by condensation of an N-terminal L-cysteine with a C-terminal L-valine residue (position one and seven, respectively, of the precursor peptide) upon reductive release of a linear heptapeptide aldehyde from the NRPS mega-enzyme by the terminal reductase of LugC (Fig. 2b and Extended Data Fig. 4d). Total chemical synthesis of lugdunin yielded a product with identical chemical properties and antimicrobial activity compared to the natural product from strain IVK28, which confirmed the assigned lugdunin structure.

The origin of lugdunin from a heptapeptide was unexpected because the NRPS proteins from the *lug* operon encompass only five adenylation domains, central enzymatic domains whose number usually determines the number of incorporated amino acids (Fig. 2b). The predicted specificities of NRPS adenylation domains[36] were in agreement with the identified amino acids, except for position three (tryptophan instead of threonine), indicating a new specificity for the second adenylation domain of LugA. Moreover, LugC exhibited an unusual modular organization[37] with one adenylation domain (valine) but two downstream peptide-bond-forming condensation and three peptidyl carrier protein domains required for amino acid transfer. This

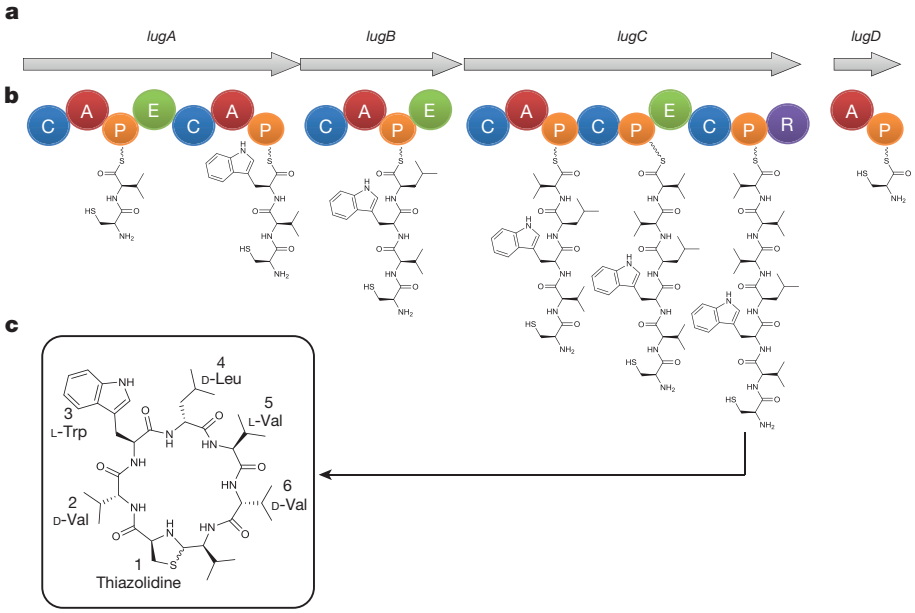

Figure 2 | Gene cluster, proposed biosynthesis pathway and chemical structure of lugdunin. a, NRPS genes *lugA*, *B*, *C*, *D*. **b**, Modular organization of gene products. Functional domains: A, adenylation; P, peptidyl carrier protein; C, condensation; E, epimerization; R, reductase. The sequential biosynthesis of lugdunin starts presumably at the characteristic initiation module of LugD and continues with LugA–C. The C-terminal reductase domain of LugC catalyses aldehyde formation at the thioester of the terminal valine and enables subsequent ring closure of the thiazolidine, leading to the cyclopeptide. **c**, Chemical structure of lugdunin. Cyclization of the reactive C-terminal aldehyde and N-terminal cysteine is assumed to occur via thiohemiacetal to the thiazolidine building block (Extended Data Fig. 4d).

organization suggested that the single adenylation domain of LugC is responsible for activation of three consecutive valine units, which are subsequently incorporated in alternating L- and D-configurations. A partially similar mechanism has been described for yersiniabactin biosynthesis[38] (see also Supplementary Discussion). Thus, the LugC domains represent an unusual assembly line compared to characterized NRPS machineries.

Activity against major human pathogens

Lugdunin has potent antimicrobial activity against a wide range of Gram-positive bacteria, including opportunistic pathogens such as difficult-to-treat methicillin-resistant *S. aureus*, glycopeptide-intermediate resistant *S. aureus* and vancomycin-resistant *Enterococcus* isolates. Minimal inhibitory concentration (MIC) values in the micromolar range (1.5–12 $\mu g\,ml^{-1}$; 1.9–15.3 μM) demonstrated high potency, and this activity was not impaired in the presence of human serum (Table 1). Lugdunin was bactericidal against methicillin-resistant *S. aureus* with complete killing at 10 × MIC (Fig. 3a). Lugdunin did not cause lysis of primary human neutrophils or erythrocytes, and even high amounts of lugdunin showed no substantial inhibition of the metabolic activity of the human monocytic cell line HL60 ($IC_{50} > 50\,\mu g\,ml^{-1}$) (Extended Data Fig. 5). Bacterial cells exposed to lugdunin stopped incorporating radioactive DNA, RNA, protein or cell-wall precursors almost simultaneously even at concentrations below the MIC (Extended Data Fig. 6), suggesting that lugdunin may lead to rapid breakdown of bacterial energy resources. In this respect, lugdunin resembles daptomycin, which has been shown to cause parallel cessation of all four metabolic pathways[39] and whose exact mode of action is still unknown. During lugdunin purification, a 2-D-*allo*-isoleucine variant (instead of 2-D-valine) was isolated. This derivative with an additional methyl group and stereogenic centre was produced by *S. lugdunensis* in small amounts and was inactive. Development of resistance was not observed in *S. aureus* during continuous serial passaging in the presence of subinhibitory concentrations of lugdunin over 30 days (Fig. 3b). In contrast, *S. aureus* rapidly developed resistance to rifampicin within a few days of exposure (Fig. 3b).

The capacity of lugdunin to cure infections *in vivo* was analysed in a mouse skin infection model reflecting a typical human *S. aureus* infection and a common indication for antibiotic treatment[40,41]. The back skin of shaved black-6 mice (C57BL/6) was superficially damaged by multiple stripping with adhesive tape and was infected with *S. aureus*. Then, 24, 30, and 42 h after infection, mice were treated with 1.5 μg lugdunin per time point and infection site, and 6 h later mice were euthanized. Lugdunin treatment led to a strong reduction or even complete eradication of viable *S. aureus* on the surface and in the deeper layers of the skin (Figs 3c, d), demonstrating that lugdunin eradicates *S. aureus* and penetrates tissues *in vivo*. Note that infection was not affected by lugdunin in two samples, most probably because some animals removed the lugdunin ointment by intensive licking. Bacteria obtained from these skin samples exhibited unchanged susceptibility to lugdunin, indicating that they had not developed resistance.

Table 1 | Lugdunin spectrum of activity

Species and strain	Resistance	Lugdunin MIC ($\mu g\,ml^{-1}$)
Staphylococcus aureus USA300 (LAC)	MRSA	1.5
+ 50% human serum		1.5
Staphylococcus aureus USA300 (NRS384)	MRSA	1.5
Staphylococcus aureus Mu50	GISA	3
Staphylococcus aureus SA113		3
Staphylococcus aureus RN4220		3
Enterococcus faecium BK463	VRE	3
Enterococcus faecalis VRE366	VRE	12
Listeria monocytogenes ATCC19118		6
Streptococcus pneumoniae ATCC49619		1.5
Bacillus subtilis 168 (*trpC2*)		4
Pseudomonas aeruginosa PAO1		>50
Escherichia coli DH5α		>50

MRSA, methicillin-resistant *S. aureus*; GISA, glycopeptide intermediate-resistant *S. aureus*; VRE, vancomycin-resistant *Enterococcus*.

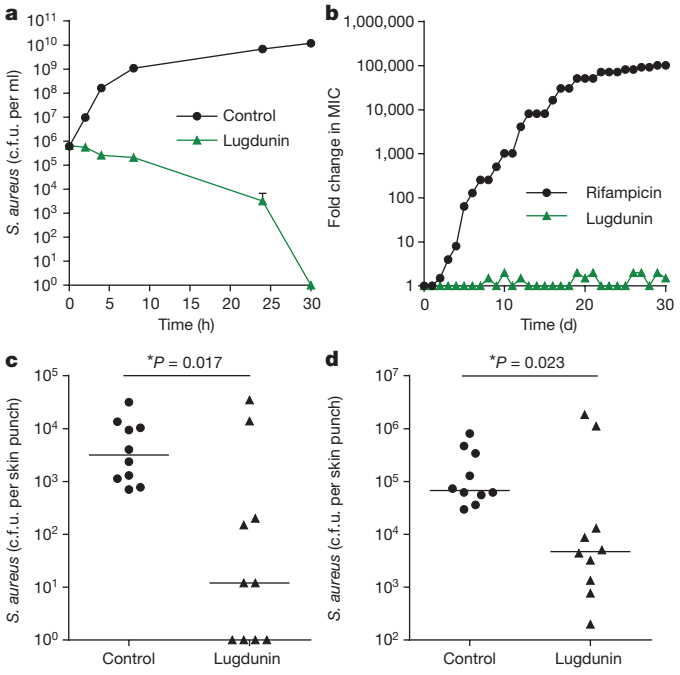

Figure 3 | Lugdunin has bactericidal activity, a low risk for resistance and efficacy in a mouse skin infection model. a, Killing curve. Incubation of *S. aureus* with a 10 × MIC of lugdunin leads to complete killing of the inoculum after 30 h (detection limit is 10° colony-forming units (c.f.u.) per ml). Data represent medians ± s.d. of three independent experiments. **b**, Serial passaging of *S. aureus* with sub-inhibitory concentrations of rifampicin leads to high resistance against rifampicin. However, development of resistance is not observed with lugdunin. A representative of two independent experiments is shown. **c**, **d**, Mouse skin infection. Lugdunin treatment (3 times, 1.5 μg per skin area) of *S. aureus* skin infections (5 mice corresponds to 10 skin punches per group) leads to strongly reduced numbers of viable bacteria after two days. c.f.u. for surface-attached bacteria (**c**) or bacteria located in the deeper skin tissue (**d**) per skin punch are shown. Horizontal lines represent the median of each group. Significant differences between groups were analysed by the Mann–Whitney test (*$P < 0.05$).

Lugdunin production outcompetes *S. aureus*

The production of antimicrobials, mostly plasmid-encoded ribosomally synthesized bacteriocins, has been sporadically documented in individual bacterial strains from human microbiota[27]. However, the roles of such compounds in microbial fitness and in microbiota dynamics have remained largely unknown. To determine whether lugdunin contributes to the capacity of *S. lugdunensis* IVK28 to prevail in competition with *S. aureus*, the two species were co-cultivated on solid agar surface, promoting lugdunin production, and bacterial numbers were monitored for three days.

As shown in Fig. 4a, the lugdunin-producing IVK28 wild type overgrew *S. aureus* efficiently, even when the inoculum contained tenfold more *S. aureus* than *S. lugdunensis* cells. No viable *S. aureus* cells were recovered after three days, indicating complete killing by *S. lugdunensis*. In contrast, IVK28 Δ*lugD* could not outcompete *S. aureus* (Fig. 4b) and was even overgrown when inoculated at tenfold higher numbers than *S. aureus* (Fig. 4d). The *S. aureus*-eradicating capacity of Δ*lugD* could be largely restored by complementation with *lugD* on a plasmid (Fig. 4c). These data demonstrate that *S. lugdunensis* IVK28 wild type can effectively eradicate *S. aureus* and that lugdunin production is responsible for this trait.

Nasal carriage is known to be a major risk factor for invasive *S. aureus* infections[19,42]. To explore whether *S. lugdunensis* can interfere with nasal *S. aureus* colonization *in vivo* in vertebrates, the noses of cotton rats, a well-established animal model for investigating *S. aureus* nasal colonization[43], were instilled with mixtures of

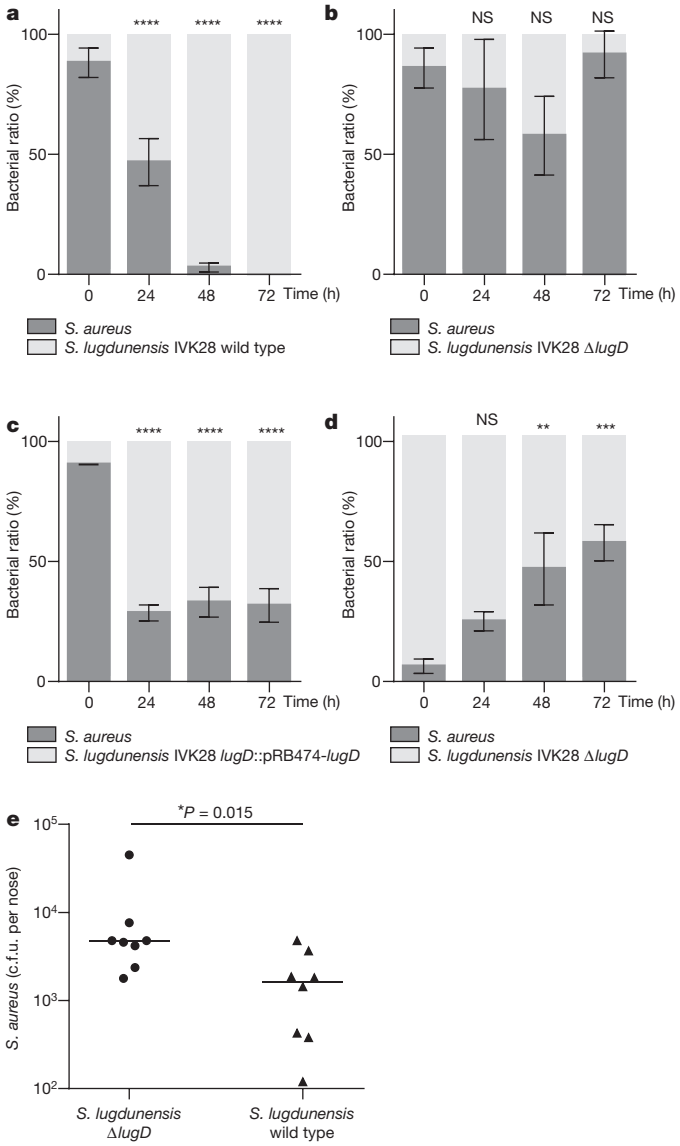

Figure 4 | Lugdunin-producing wild-type *S. lugdunensis* IVK28 restricts the growth of *S. aureus in vitro* and *in vivo* in cotton rats. **a**, *S. aureus* is overgrown by wild-type *S. lugdunensis* IVK28 (dark or light grey columns, respectively) on agar plates inoculated at ratios of ~90:10. **b**, In contrast, the ratio between IVK28 Δ*lugD* and *S. aureus*, inoculated at a ratio of ~90:10, does not change significantly over time. **c**, The capacity of *S. lugdunensis* Δ*lugD* to overgrow *S. aureus* is largely restored by plasmid-encoded *lugD*. **d**, *S. aureus* displaces IVK28 Δ*lugD* even when inoculated at ratios of ~10:90. Data represent mean values ± s.d. of three independent experiments. Significant differences between starting conditions and indicated time points were analysed by one-way ANOVA (*$P < 0.05$; **$P < 0.01$; ***$P < 0.001$; ****$P < 0.0001$; NS, not significant). **e**, Cotton rat noses (8 animals per group) co-colonized by *S. aureus* and *S. lugdunensis* IVK28 wild type show significantly less *S. aureus* c.f.u. after five days compared to *S. lugdunensis* IVK28 Δ*lugD*. Horizontal lines represent the median of each group. Significant differences, calculated by the Mann–Whitney test, are indicated (*$P < 0.05$).

S. lugdunensis IVK28 wild type or Δ*lugD* plus *S. aureus*. The three test strains colonized cotton rat noses stably over the 5-day test period when instilled individually (Extended Data Fig. 7). However, when the two species were co-inoculated, significantly less *S. aureus* cells were retrieved from animals co-colonized by IVK28 wild type compared to those co-colonized with Δ*lugD* (Fig. 4e). This finding indicates that lugdunin production can effectively interfere with *S. aureus* colonization *in vivo*.

Table 2 | *S. aureus* and *S. lugdunensis* distribution in hospitalized patients

	S. lugdunensis-positive	*S. lugdunensis*-negative	Total
S. aureus-positive	1	59	60
S. aureus-negative	16	111	127
Total	17	170	187
Risk§	0.059*	0.347*	0.321

Significant differences between *S. lugdunensis*-positive and *S. lugdunensis*-negative patients were analysed by the Chi-squared test.
§0.059 versus 0.347: risk ratio, 0.169; 95% confidence interval 0.025–1.147.
*$P = 0.015$.

Interference with *S. aureus* carriage

Factors governing human nasal *S. aureus* carrier status have remained largely unknown[42,44]. To investigate whether the presence of *S. lugdunensis* in the human nose can prevent co-colonization by *S. aureus*, we examined nasal swabs from 187 hospitalized patients for colonization by *S. lugdunensis, S. aureus* or both. The overall colonization rates of *S. aureus* and *S. lugdunensis* were 32.1% and 9.1%, respectively (Table 2), which corresponds to published data[20,45]. Of note, the percentage of *S. aureus* colonization in *S. lugdunensis*-positive individuals (5.9%) was approximately 5.9-fold lower than in *S. lugdunensis*-negative individuals (34.7%). Chi-squared statistical analysis showed that the reduced *S. aureus* detection rate in the presence of *S. lugdunensis* for the entire study population was significant (risk ratio 0.169; 95% confidence interval 0.025–1.147; $P = 0.015$; Table 2) indicating that strong interference precludes the simultaneous presence of *S. aureus* and *S. lugdunensis* in the human nose. Consistent with this finding, PCR analysis demonstrated that all nasal *S. lugdunensis* isolates contained the *lug* operon and all of the tested *S. aureus* strains (30 nasal as well as 7 laboratory) were found to be highly susceptible to lugdunin. Together with the ability of the lugdunin producer IVK28 to reduce *S. aureus* numbers in cotton rat noses, these data provide strong evidence for the potent capacity of *S. lugdunensis* to prevent human nasal colonization by *S. aureus*.

Conclusions

The human predisposition to *S. aureus* nasal carriage is governed by several host genetic or microbiota-related factors, which may affect the capacity of *S. aureus* to adhere to and multiply on nasal epithelia[43,44,46]. Here we provide evidence for a crucial role of *S. lugdunensis* and its antimicrobial product, lugdunin, in preventing *S. aureus* colonization of the human nose. *S. aureus* can only rarely be isolated from the axillae or groin, also habitats of *S. lugdunensis* in addition to nares[45], which may therefore be related to the production of lugdunin at these sites. Accordingly, utilizing lugdunin or lugdunin-producing commensal staphylococci could become a valuable strategy for preventing *S. aureus* colonization and invasive infections in high-risk patients, such as those undergoing elective surgery, immunosuppression, or regular haemodialysis. The concept of probiotic bacteria interfering with predisposition to infection has been pursued mostly for enteric pathogens[47]. Our study suggests that the probiotics concept should be extended to body sites other than the gut, such as the nasal mucous membranes, and to additional major pathogens such as *S. aureus*. *S. lugdunensis* is known as a rare cause of opportunistic infections[48], but a mutant lacking all potential virulence factors or introduction of the *lug* genes into an exclusively commensal species might enable the development of a safe probiotic strain.

Lugdunin represents the first example, to our knowledge, of a new class of compounds that we suggest should be named macrocyclic thiazolidine peptide antibiotics. Lugdunin shows bactericidal activity against many major pathogens combined with a particularly high barrier to resistance by mutation, even under prolonged selective pressure. The fact that all tested nasal and clinical *S. aureus* isolates maintained pronounced susceptibility to lugdunin suggests that it may be particularly difficult for bacteria to develop resistance to lugdunin. This indicates that lugdunin has apparently evolved for the purpose of bacterial elimination in the human organism, implying that it is optimized for efficacy and tolerance at its physiological site of action. Thus, lugdunin shows promise as a potential drug for inhibiting growth of *S. aureus* in the nares and potentially other body sites.

The genetic inventory of human-associated microbiomes is of great importance for many critical human body functions for example, degradation of ingested polymers, detoxification of xenobiotics, and release of immunomodulatory molecules[49]. Our discovery of commensal bacteria producing a potent antibiotic is in accord with recent reports on the presence of gene clusters for complex secondary metabolites in human-associated metagenomes[30] and suggests that many humans are constantly exposed to potent bioactive compounds from microbiota. The effect of such compounds on human body functions may vary substantially with the dynamic changes in microbiota structure. Whereas it has become increasingly difficult to identify novel compound structures from soil microbes such as actinomycetes, bacteria from human microbiota may become a valuable source for new types of antibiotics. It will be a challenge for future research to elucidate the identity, variability, activity, and ecological roles of such compounds and to exploit them for the development of new drugs.

Online Content Methods, along with any additional Extended Data display items and Source Data, are available in the online version of the paper; references unique to these sections appear only in the online paper.

Received 12 November 2015; accepted 9 June 2016.

1. Arias, C. A. & Murray, B. E. Antibiotic-resistant bugs in the 21st century—a clinical super-challenge. *N. Engl. J. Med.* **360,** 439–443 (2009).
2. Laxminarayan, R. *et al.* Antibiotic resistance—the need for global solutions. *Lancet Infect. Dis.* **13,** 1057–1098 (2013).
3. DeLeo, F. R., Otto, M., Kreiswirth, B. N. & Chambers, H. F. Community-associated meticillin-resistant *Staphylococcus aureus*. *Lancet* **375,** 1557–1568 (2010).
4. Arias, C. A. & Murray, B. E. The rise of the *Enterococcus*: beyond vancomycin resistance. *Nat. Rev. Microbiol.* **10,** 266–278 (2012).
5. Boucher, H. W. *et al.* Bad bugs, no drugs: no ESKAPE! An update from the Infectious Diseases Society of America. *Clin. Infect. Dis.* **48,** 1–12 (2009).
6. WHO. Antimicrobial resistance: global report on surveillance 2014. http://www.who.int/drugresistance/documents/surveillancereport/en/ (2014).
7. Cooper, M. A. & Shlaes, D. Fix the antibiotics pipeline. *Nature* **472,** 32 (2011).
8. Bierbaum, G. & Sahl, H. G. The search for new anti-infective drugs: untapped resources and strategies. *Int. J. Med. Microbiol.* **304,** 1–2 (2014).
9. Ling, L. L. *et al.* A new antibiotic kills pathogens without detectable resistance. *Nature* **517,** 455–459 (2015).
10. Laureti, L. *et al.* Identification of a bioactive 51-membered macrolide complex by activation of a silent polyketide synthase in *Streptomyces ambofaciens*. *Proc. Natl Acad. Sci. USA* **108,** 6258–6263 (2011).
11. Hosaka, T. *et al.* Antibacterial discovery in actinomycetes strains with mutations in RNA polymerase or ribosomal protein S12. *Nat. Biotechnol.* **27,** 462–464 (2009).
12. Lincke, T., Behnken, S., Ishida, K., Roth, M. & Hertweck, C. Closthioamide: an unprecedented polythioamide antibiotic from the strictly anaerobic bacterium *Clostridium cellulolyticum*. *Angew. Chem. Int. Ed. Engl.* **49,** 2011–2013 (2010).
13. Schroeder, B. O. *et al.* Reduction of disulphide bonds unmasks potent antimicrobial activity of human β-defensin 1. *Nature* **469,** 419–423 (2011).
14. Zasloff, M. Inducing endogenous antimicrobial peptides to battle infections. *Proc. Natl Acad. Sci. USA* **103,** 8913–8914 (2006).
15. Bush, K. *et al.* Tackling antibiotic resistance. *Nat. Rev. Microbiol.* **9,** 894–896 (2011).
16. Marshall, B. M. & Levy, S. B. Food animals and antimicrobials: impacts on human health. *Clin. Microbiol. Rev.* **24,** 718–733 (2011).
17. Penders, J., Stobberingh, E. E., Savelkoul, P. H. & Wolffs, P. F. The human microbiome as a reservoir of antimicrobial resistance. *Front. Microbiol.* **4,** 87 (2013).
18. Davis, M. F., Price, L. B., Liu, C. M. & Silbergeld, E. K. An ecological perspective on U.S. industrial poultry production: the role of anthropogenic ecosystems on the emergence of drug-resistant bacteria from agricultural environments. *Curr. Opin. Microbiol.* **14,** 244–250 (2011).
19. Bode, L. G. *et al.* Preventing surgical-site infections in nasal carriers of *Staphylococcus aureus*. *N. Engl. J. Med.* **362,** 9–17 (2010).
20. Wertheim, H. F. *et al.* The role of nasal carriage in *Staphylococcus aureus* infections. *Lancet Infect. Dis.* **5,** 751–762 (2005).
21. Thomas, C. M., Hothersall, J., Willis, C. L. & Simpson, T. J. Resistance to and synthesis of the antibiotic mupirocin. *Nat. Rev. Microbiol.* **8,** 281–289 (2010).

22. van der Meer, J. W. & Vandenbroucke-Grauls, C. M. Resistance to selective decontamination: the jury is still out. *Lancet Infect. Dis.* **13,** 282–283 (2013).
23. Schloss, P. D. Microbiology: An integrated view of the skin microbiome. *Nature* **514,** 44–45 (2014).
24. Laufer, A. S. *et al.* Microbial communities of the upper respiratory tract and otitis media in children. *MBio* **2,** e00245–e10 (2011).
25. Krismer, B. *et al.* Nutrient limitation governs Staphylococcus aureus metabolism and niche adaptation in the human nose. *PLoS Pathog.* **10,** e1003862 (2014).
26. Hibbing, M. E., Fuqua, C., Parsek, M. R. & Peterson, S. B. Bacterial competition: surviving and thriving in the microbial jungle. *Nat. Rev. Microbiol.* **8,** 15–25 (2010).
27. Dobson, A., Cotter, P. D., Ross, R. P. & Hill, C. Bacteriocin production: a probiotic trait? *Appl. Environ. Microbiol.* **78,** 1–6 (2012).
28. Kommineni, S. *et al.* Bacteriocin production augments niche competition by enterococci in the mammalian gastrointestinal tract. *Nature* **526,** 719–722 (2015).
29. Challinor, V. L. & Bode, H. B. Bioactive natural products from novel microbial sources. *Ann. NY Acad. Sci.* **1354,** 82–97 (2015).
30. Donia, M. S. *et al.* A systematic analysis of biosynthetic gene clusters in the human microbiome reveals a common family of antibiotics. *Cell* **158,** 1402–1414 (2014).
31. Heilbronner, S. *et al.* Genome sequence of *Staphylococcus lugdunensis* N920143 allows identification of putative colonization and virulence factors. *FEMS Microbiol. Lett.* **322,** 60–67 (2011).
32. Sidda, J. D. *et al.* Discovery of a family of gamma-aminobutyrate ureas via rational derepression of a silent bacterial gene cluster. *Chem. Sci.)* **5,** 86–89 (2014).
33. Rutledge, P. J. & Challis, G. L. Discovery of microbial natural products by activation of silent biosynthetic gene clusters. *Nat. Rev. Microbiol.* **13,** 509–523 (2015).
34. Sasaki, O., Igarashi, Y., Saito, N. & Furumai, T. Watasemycins A and B, new antibiotics produced by *Streptomyces* sp. TP-A0597. *J Antibiot. (Tokyo)* **55,** 249–255 (2002).
35. Miller, D. A., Luo, L., Hillson, N., Keating, T. A. & Walsh, C. T. Yersiniabactin synthetase: a four-protein assembly line producing the nonribosomal peptide/polyketide hybrid siderophore of *Yersinia pestis*. *Chem. Biol.* **9,** 333–344 (2002).
36. Weber, T. *et al.* antiSMASH 3.0-a comprehensive resource for the genome mining of biosynthetic gene clusters. *Nucleic Acids Res.* **43,** W237–W243 (2015).
37. Walsh, C. T. Insights into the chemical logic and enzymatic machinery of NRPS assembly lines. *Nat. Prod. Rep.* **33,** 127–135 (2015).
38. Mootz, H. D., Schwarzer, D. & Marahiel, M. A. Ways of assembling complex natural products on modular nonribosomal peptide synthetases. *ChemBioChem* **3,** 490–504 (2002).
39. Hobbs, J. K., Miller, K., O'Neill, A. J. & Chopra, I. Consequences of daptomycin-mediated membrane damage in *Staphylococcus aureus*. *J. Antimicrob. Chemother.* **62,** 1003–1008 (2008).
40. Tacconelli, E. & Kern, W. V. New antibiotics for skin and skin-structure infections. *Lancet Infect. Dis.* **14,** 659–661 (2014).
41. Zervos, M. J. *et al.* Epidemiology and outcomes of complicated skin and soft tissue infections in hospitalized patients. *J. Clin. Microbiol.* **50,** 238–245 (2012).
42. Weidenmaier, C., Goerke, C. & Wolz, C. *Staphylococcus aureus* determinants for nasal colonization. *Trends Microbiol.* **20,** 243–250 (2012).
43. Baur, S. *et al.* A nasal epithelial receptor for *Staphylococcus aureus* WTA governs adhesion to epithelial cells and modulates nasal colonization. *PLoS Pathog.* **10,** e1004089 (2014).
44. Andersen, P. S. *et al.* Influence of host genetics and environment on nasal carriage of *Staphylococcus aureus* in Danish middle-aged and elderly twins. *J. Infect. Dis.* **206,** 1178–1184 (2012).
45. Bieber, L. & Kahlmeter, G. *Staphylococcus lugdunensis* in several niches of the normal skin flora. *Clin. Microbiol. Infect.* **16,** 385–388 (2010).
46. Iwase, T. *et al. Staphylococcus epidermidis* Esp inhibits *Staphylococcus aureus* biofilm formation and nasal colonization. *Nature* **465,** 346–349 (2010).
47. Sanders, M. E. Impact of probiotics on colonizing microbiota of the gut. *J. Clin. Gastroenterol*. **45** (Suppl), S115–S119 (2011).
48. Becker, K., Heilmann, C. & Peters, G. Coagulase-negative staphylococci. *Clin. Microbiol. Rev.* **27,** 870–926 (2014).
49. Clemente, J. C., Ursell, L. K., Parfrey, L. W. & Knight, R. The impact of the gut microbiota on human health: an integrative view. *Cell* **148,** 1258–1270 (2012).

Supplementary Information is available in the online version of the paper.

Acknowledgements We thank V. Winstel for technical assistance and A. Bobic, S. Heilbronner, W. Hoffmann, A. Jorge, D. Kretschmer, A. Kulik, M. Nega, E. Stegmann, V. Winstel, T. Weber, and W. Wohlleben for assistance and helpful discussions. Thanks to Bruker Daltonics for selected initial high-resolution mass spectrometry analysis and to T. Paululat for NMR experiments. This work was financed by German Research Council grants GRK1708 to S.G. and A.P.; TRR156, Schi510/8-1, and PE805/5-1 to B.S. and A.P.; TRR34 to C.W. and A.P; and SFB766 to C.W., H.B.-O., S.G., and A.P.; and by the German Center for Infection Research (DZIF) to C.W., A.P., B.K., M.W., and H.B.-O.

Author Contributions A.Z. isolated lugdunin, designed experiments and investigated the biological activities of lugdunin. M.C.K. purified lugdunin, designed experiments and determined the structure of lugdunin. D.J. identified IVK28 and performed transposon mutagenesis. A.B. designed and performed precursor incorporation studies. C.L. designed the human colonization study and analysed data. M.B., A.Z., C.S. and C.W. performed animal experiments, and M.W. and C.W. analysed data and performed statistical analysis. M.M. provided patient samples and supported MALDI-TOF analysis. N.A.S. and H.K. established total chemical synthesis of lugdunin. B.K. isolated lugdunin, analysed operon structure and performed bioinformatic analyses, A.Z., M.C.K., B.S., H.B.-O., S.G., A.P. and B.K. designed the study, analysed results, and wrote the paper.

Author Information Reprints and permissions information is available at www.nature.com/reprints. The authors declare competing financial interests: details are available in the online version of the paper. Readers are welcome to comment on the online version of the paper. Correspondence and requests for materials should be addressed to A.P. (andreas.peschel@uni-tuebingen.de).

Reviewer Information *Nature* thanks G. Challis, M. Gilmore and K. Lewis for their contribution to the peer review of this work.

METHODS

Data reporting. The animal experiments were not randomized and the investigators were not blinded to allocation during experiments and outcome assessment. No statistical methods were used to predetermine sample size. For the human colonization study, only anonymous and randomized samples were obtained.

Strains and growth conditions. The *Staphylococcus* strains used in this study were *S. aureus* USA300 LAC, *S. aureus* USA300 NRS384, *S. aureus* Mu50, *S. aureus* RN4220, *S. aureus* SA113, *S. aureus* Newman, *S. aureus* PS187, *S. lugdunensis* IVK28, *S. lugdunensis* IVK28 Δ*lugD*, and *S. lugdunensis* IVK28-Xyl. Further strains used for MIC determination were *Enterococcus faecium* BK463, *E. faecalis* VRE366, *Listeria monocytogenes* ATCC19118, *Streptococcus pneumoniae* ATCC49619, *Pseudomonas aeruginosa* PAO1, and *Escherichia coli* DH5α. *E. coli* DC10B was used as the cloning host and *B. subtilis* 168 (*trpC2*) was used for precursor incorporation studies. In addition, a set of 60 *S. aureus* and 17 *S. lugdunensis* strains were isolated from diagnostic samples in the course of the colonization study described below.

Basic medium (BM: 1% soy peptone, 0.5% yeast extract, 0.5% NaCl, 0.1% glucose and 0.1% K_2HPO_4, pH 7.2) was used as the standard growth medium. MIC determinations and killing assays were performed in Mueller Hinton Broth (MHB; Roth, Karlsruhe, Germany). For the identification of *S. lugdunensis*, selective *S. lugdunensis* medium (SSL) was used as previously described[50]. When necessary, antibiotics were used at concentrations of 250 μg ml^{-1} for streptomycin, 10 μg ml^{-1} for chloramphenicol, 2.5 μg ml^{-1} for erythromycin, and 100 μg ml^{-1} for ampicillin.

Bioactivity test. The antimicrobial activity against *S. aureus* of *S. lugdunensis* IVK28 was identified by screening 90 nasal staphylococcal isolates for the capacity to inhibit growth of *S. aureus*. For this purpose, BM agar was inoculated 1:10,000 with an overnight culture of *S. aureus* USA300 LAC. The test strains were inoculated on the resulting bacterial lawn, and the plates were incubated for 24–48 h at 37 °C. To investigate the production of antimicrobial activity by IVK28 under iron-limiting conditions, BM agar was supplemented with 200 μM 2, 2'-bipyridine[25].

Transposon mutagenesis and elucidation of the lugdunin gene cluster. The temperature-sensitive plasmid pTV1ts, which contains the 5.3-kb transposon *Tn*917 (*erm*^{R}) from *E. faecalis*, was transferred into *S. lugdunensis* IVK28 by electroporation. Transposon mutants were screened for loss of antimicrobial activity against *S. aureus*. Chromosomal DNA was isolated by standard procedures from non-inhibitory clones, and the primers Tn917 up and Tn917 down (Extended Table 2) were used to directly sequence the flanking regions of the transposon insertion site. Sequence analysis was performed with DNASTAR Lasergene software (DNASTAR Inc., Madison, WI, USA). Bioinformatic analysis was performed by BLAST (http://blast.ncbi.nlm.nih.gov/Blast.cgi) and antiSMASH 3.0 (ref. 36).

Generation of *S. lugdunensis* IVK28-Xyl. The flanking regions of *lugR* were amplified by PCR with the primer pairs SIPr1–up/SIPr1–down and SIPr2–up/SIPr2–down (Extended Data Table 2). The plasmid pBASE6-erm/lox 1, a derivative of pBASE6 (ref. 51), already containing an erythromycin resistance cassette in the singular SmaI site, was linearized with Acc65I. The identically digested SIPr1 PCR product, containing one natural Acc65I restriction site and one introduced by the primer, was ligated into pBASE6-erm/lox1. The resulting vector with the correctly oriented SIPr1 PCR product and the SIPr2 PCR product were ligated after digestion with EcoRV and BglII. The resulting pBASE6-erm/lox 1 construct with both flanking regions inserted was linearized with BssHII, treated with Klenow enzyme and digested with BgII. The required *xylR* fragment with the downstream-located *xylAB*-promoter was excised from pTX15 by HindIII restriction, treated with Klenow enzyme and subsequently digested with BamHI. The ligation of the *xylR* fragment into the appropriate vector generated pBASE6-erm/lox1-*xylR*, which was transferred into *E.coli* DC10B and subsequently into *S. aureus* PS187. The resulting plasmid pBASE6-erm/lox1-*xylR* was transduced into *S. lugdunensis* IVK28 via the bacteriophage Φ187 according to ref. 52. Homologous recombination for replacement of *lugR* by *erm/xylR* was performed as previously described[51], generating the xylose-inducible lugdunin producer strain *S. lugdunensis* IVK28-Xyl.

Production and purification of lugdunin. A fresh overnight culture of *S. lugdunensis* IVK28-Xyl was inoculated 1:1,000 in BM without glucose and was supplemented with 0.5% xylose. After incubation at 37 °C under continuous shaking (160 rpm) for 24 h, whole cultures were extracted with 1-butanol at a ratio of 5:1. The aqueous phase was discarded, and the organic phase was evaporated at 37 °C under reduced pressure and finally dissolved in methanol. The methanol extract was applied to a gel filtration column (Sephadex LH20, 1.6 × 80 cm, flow rate 1 ml min^{-1} methanol). The active fractions containing lugdunin were pooled, evaporated at 37 °C under reduced pressure and dissolved in dimethyl sulfoxide (DMSO). This solution was then subjected to a preparative reversed-phase HPLC column (Kromasil C18, 7 μm, 250 × 20 mm; Dr. Maisch, Ammerbuch, Germany) with an isocratic elution at 79% methanol in water for 20 min. The fractions containing lugdunin were baseline-separated from the remaining compounds. Methanol was evaporated at 37 °C under reduced pressure to yield lugdunin as a white powder.

Chemical synthesis of lugdunin. Total chemical synthesis was achieved by a Fmoc (9-fluorenylmethoxycarbonyl) strategy-based manual solid-phase peptide synthesis and was established on an H-Val-H NovaSyn TG resin (Novabiochem, Switzerland). Amino acids were coupled in a fourfold excess using HATU (1-[bis(dimethylamino)methylene]-1*H*-1,2,3-triazolo[4,5-*b*]pyridinium 3-oxid hexafluorophosphate). Valine positions were coupled twice by PyOxim ([ethyl cyano(hydroxyimino)acetato-*O*^{2}]tri-1-pyrrolidinylphosphonium hexafluorophosphate) for the second coupling instead of HATU. Deprotection was performed in trifluoroacetic acid for 30 min. Peptides were cleaved from the resin with acetonitrile:water:trifluoroacetic acid (79.95:20:0.05) for 30 min. Lyophilisation yielded the crude product. Crude synthetic lugdunin product was purified by reversed-phase HPLC and compared with the natural product by electrospray ionization liquid chromatography high-resolution mass spectrometry, additional chiral-HPLC methods (column, Dr. Maisch Reprosil Chiral NR, Ammerbuch, Germany; elution with 80% premixed methanol in H_2O at 1.5 ml min^{-1} flow rate), bioactivity assay and advanced Marfey's analysis.

MIC assay, serum stability and spectrum of activity. *S. aureus* RN4220, *S. aureus* USA300 (LAC), *S. aureus* USA300 (NRS384), *S. aureus* SA113, *S. aureus* Mu50, *E. coli* DH5α and *P. aeruginosa* PAO1 were grown overnight in MHB. *E. faecalis* VRE366, *E. faecium* BK463, *S. pneumoniae*, and *L. monocytogenes* were grown in tryptic soy broth (Difco Laboratories, Augsburg, Germany). Serum stability of lugdunin was determined in 50% MHB with 50% human serum, which was obtained by standard Histopaque/Ficoll centrifugation of freshly isolated blood. All strains were incubated at 37 °C under continuous shaking. Early log-phase grown bacteria were adjusted in MHB to 1 × 10^6 c.f.u. per ml in microtiter plates, mixed with varying concentrations of the antibiotic and incubated at 37 °C for 24 h under continuous shaking. The OD_{600} of each well was measured with a microplate reader, and the lowest peptide concentrations, which displayed no bacterial growth, were defined as the MIC. The assays were performed in 96-well microtiter plates. MIC values for *B. subtilis* 168 to be used as points of reference in precursor incorporation studies were determined in Belitzky minimal medium[53], using a final inoculum of 5 × 10^5 c.f.u. per ml.

Killing assay. Fresh MHB was inoculated 1:10,000 with an overnight culture of *S. aureus* USA300 LAC and was incubated at 37 °C under continuous shaking (160 rpm) until bacteria were grown to 1 × 10^6 c.f.u. per ml. Then, 10 × MIC lugdunin was added. At the time points 0 h, 2 h, 4 h, 8 h, 24 h and 30 h, samples were taken and centrifuged. The pellet was resuspended in 1 × PBS and serially diluted. The dilutions were spotted on tryptic soy agar, and colony counts were determined after overnight incubation at 37 °C. To determine cell numbers <10^2 c.f.u. per ml, whole cultures were centrifuged and plated on tryptic soy agar.

Precursor incorporation studies. *B. subtilis* 168 (*trpC2*) is a widely used model organism for mode of action investigations and was also used for orienting studies on the mechanism of lugdunin[54–56]. To measure incorporation of radioactive precursors into acid-precipitable macromolecules, *B. subtilis* 168 (*trpC2*), exponentially growing in Belitzky minimal medium (OD_{600} of 0.04), was labelled with 0.02 MBq ml^{-1} of [methyl-^{3}H]thymidine (DNA synthesis), [5,6-^{3}H]uridine (RNA synthesis), [4,5-^{3}H]L-leucine (protein synthesis) or [1-^{3}H]glucosamine D-hydrochloride (cell-wall synthesis). After 5 min culture aliquots were treated with lugdunin at concentrations of 2, 1, 0.67 or 0.5 μg ml^{-1}, corresponding to 1/2×, 1/4×, 1/6× or 1/8× the MIC, respectively. Ciprofloxacin (2 μg ml^{-1}, 4 × MIC), rifampicin (1 μg ml^{-1}, 4 × MIC), chloramphenicol (16 μg ml^{-1}, 4 × MIC) or vancomycin (2 μg ml^{-1}, 4 × MIC) served as reference antibiotics for inhibition of DNA, RNA, protein or cell-wall biosynthesis, respectively. Samples (0.1 ml) were taken in regular time intervals and precipitated with 6% perchloric acid in a multiscreen filter plate (Millipore, 0.45 μm). After washing the precipitates with 0.15 ml of ethanol, plates were dried and radioactivity was determined with scintillation fluid (Ultima Gold, Perkin Elmer) in a 1450 MicroBeta TriLux counter (Wallac).

Cytotoxicity against eukaryotic cells. Human neutrophil granulocytes were freshly isolated from the blood of healthy volunteers by standard Histopaque/Ficoll centrifugation. Lysis of neutrophil granulocytes was monitored by the release of the enzyme lactate dehydrogenase (LDH), as described in ref. 57. Lugdunin was added at final concentrations of 50, 25 and 12.5 μg ml^{-1} in 0.5% DMSO to wells of a 96-well tissue culturing plate containing 1 × 10^6 neutrophil granulocytes per well in 200 μl RPMI-1640 medium (2 g l^{-1} $NaHCO_3$, 10% foetal calf serum, 1% L-glutamine and 1% penicillin-streptomycin, PAN Biotech) without phenol red. The plates were incubated at 37 °C and 5% CO_2 for 3 h and the lysis was determined with the LDH Cytotoxicity Detection Kit (Roche Applied Sciences, Mannheim, Germany).

Haemolytic activity was determined with human erythrocytes, freshly isolated from the blood of healthy volunteers by standard Histopaque/Ficoll centrifugation. Lugdunin was added at final concentrations of 50, 25 and 12.5 μg ml^{-1} in 0.5% DMSO to 2% erythrocytes in 1 × PBS. The cells were incubated for 1 h and afterwards centrifuged for 10 min at 1,000 rpm. The supernatant was diluted 1:10 in 1 × PBS, and the absorbance was measured at a wavelength of 540 nm. As a positive control for neutrophil granulocyte or erythrocyte lysis, 2% Triton X-100 was added to the samples.

HL60 cells were cultured in RPMI-1640 medium. Their metabolic activity was monitored using the cell health indicator alamarBlue (Invitrogen) as described in ref. 58. Lugdunin was added at final concentrations of 50, 25 and 12.5 μg ml^{-1} in 0.5% DMSO to wells of a 96-well tissue culturing plate containing 1×10^4 HL60 cells per well. The plates were incubated at 37 °C and 5% CO_2 for 24 h. As a positive control for high cytotoxicity, staurosporine was added to the samples. The HL60 cell line, which we have obtained from CNRS (Université Grenoble, France), and whose identity was confirmed by the provider, is not listed in the database as commonly misidentified. Mycoplasma assays were negative.

Resistance development study. MIC assays for the antibiotics used in this study were performed as described above. We determined 1 × MICs of 0.01 μg ml^{-1} rifampicin and 1.5 μg ml^{-1} lugdunin against *S. aureus* USA300. Fresh MHB was inoculated 1:10,000 with an overnight culture of *S. aureus* USA300 LAC and was incubated at 37 °C under continuous shaking. Cells were grown to early log phase, adjusted to 1×10^6 cells ml^{-1}, and dispensed into 96-well microtiter plates with 100 μl per well. Lugdunin and rifampicin were added at concentrations of 0.25×, 0.5×, 1×, 1.5×, 2× and 4× MIC. After 24 h incubation at 37 °C under continuous shaking, growth was determined with a microplate reader at an OD_{600}, and cells from the second highest concentration showing visible growth were used to inoculate the subsequent culture.

Statistical analyses. Statistical analysis was performed by using GraphPad Prism (GraphPad Software, Inc., La Jolla, USA; version 5.04). Statistically significant differences were calculated by appropriate statistical methods as indicated. For the human study, risk of nasal colonization with *S. aureus* in the presence or absence of *S. lugdunensis*, as well as the respective point estimates of the risk ratio and confidence intervals, were determined using Stata version 12.1 (Stat Corp., College Station, TX, USA). *P* values of ≤ 0.05 were considered significant.

Animal models and ethics statement. All animal experiments were conducted in strict accordance with the German regulations of the Gesellschaft für Versuchstierkunde/Society for Laboratory Animal Science (GV-SOLAS) and the European Health Law of the Federation of Laboratory Animal Science Associations (FELASA) in accordance with German laws after approval (protocol HT1/12 for mouse skin infection and T1/10 for cotton rat colonization) by the local authorities (Regierungspräsidium Tübingen). All, animal and human studies were carried out at the University Hospital Tübingen and conformed to institutional animal care and use policies. No randomization or blinding was necessary for the animal infection/colonization models, and no samples were excluded. Animal studies were performed with female C57BL/6 mice, 6–8 weeks old, or cotton rats of both genders, 8–10 weeks old, respectively. The human nasal colonization study was approved by the ethics committee of the medical faculty of the University Hospital Tübingen (project number 577/2015A).

Skin infection of C57BL/6 mice. A streptomycin-resistant *S. aureus* Newman strain was used to infect C57BL/6 mice epicutaneously by the tape-stripping technique from ref. 59. Tryptic soy broth with 500 μg ml^{-1} streptomycin was inoculated 1:10,000 with a fresh overnight culture of the test strain and was incubated at 37 °C under continuous shaking until an OD_{600} of 0.5 was reached. Cells were centrifuged, washed twice with 1 × PBS, and adjusted to 1×10^8 cells per ml. The integrity of the shaved skin of the mice was affected by repeated (seven times) vigorous tape stripping to enable *S. aureus* Newman infection. An inoculum of 15 μl from the bacterial suspension was added to 7-mm filter paper discs, placed onto the prepared skin with two discs per animal, and covered with Finn chambers on Scanpor tape (Smart Practise, Phoenix, AZ, USA). Finn chamber fixation occurred via Fixomull stretch plasters (BSN medical GmbH, Hamburg, Germany). After incubation for 24 h, the Finn chambers were removed and 1.5 μg of lugdunin per colonized area was applied, followed by a second and third treatment with the same amount of lugdunin after 30 h and 42 h. Six hours after the final application, mice were euthanized, the skin was large-scale detached and 4-mm punches of the originally colonized areas were vortexed in 1 × PBS for 30 s to remove the attached bacteria from the skin (wash fraction). The skin was dissected with a scalpel to expose bacteria from deeper areas of the skin (tissue fraction), which was homogenized by vortexing in 1 × PBS for 30 s. c.f.u. of both fractions were determined by serial dilutions in 1 × PBS, which were spotted onto tryptic soy agar, supplemented with streptomycin, for a streptomycin-resistant *S. aureus* Newman-specific selection. The plates were incubated overnight at 37 °C.

Generation of *S. lugdunensis* Δ*lugD* and complementation. For the construction of a marker-less knockout strain, 1-kb flanking regions of *lugD* were amplified by PCR with the primer pairs *lugD* upstream-SacI/*lugD* upstream-Acc65I and *lugD* downstream-Acc65I/*lugD* downstream-BglII (Extended Data Table 2). The fragments were digested according to their introduced restriction sites and were ligated into the plasmid pBASE6 generating pBASE6-Δ*lugD*, which was transferred to *E. coli* DC10B. The correct plasmid was transferred to *S. aureus* PS187 by electroporation, which was then infected with the bacteriophage Φ187 for the transduction of pBASE6-Δ*lugD* into *S. lugdunensis* IVK28 wild type. The knockout was generated by homologous recombination of the flanking regions into the genome, and deletion of *lugD* was confirmed by PCR. For the complementation of the mutant, *lugD* was amplified by the primer pair *lugD* complementation forward-PstI/*lugD* complementation reverse-Acc65I (Extended Data Table 2), digested with the appropriate restriction enzymes and ligated into identically digested pRB474. The resulting pRB474-*lugD* was transduced into *S. lugdunensis* IVK28 Δ*lugD*, as described for the knockout mutant.

Competition assay. *S. lugdunensis* IVK28 wild type, *S. lugdunensis* IVK28 Δ*lugD*, *S. lugdunensis* IVK28 Δ*lugD*::pRB474-lugD, and a streptomycin-resistant *S. aureus* Newman were grown in BM overnight at 37 °C under continuous shaking. These strains were then adjusted to 1×10^9 c.f.u. per ml in 1 × PBS and diluted 1:10. For the starting condition of 90% *S. aureus*, equal volumes of 1×10^9 *S. aureus* c.f.u. per ml and 1×10^8 *S. lugdunensis* c.f.u. per ml were mixed. Co-cultures with only 10% *S. aureus* were also performed, and 20 μl of these mixtures were spotted in triplicate on BM agar and incubated at 37 °C. Samples were taken at 0 h, 24 h, 48 h, and 72 h by scraping cells from the agar plates and suspending them in 1 × PBS. Serial dilutions of these samples were plated on BM and BM containing streptomycin for selection of *S. aureus*. After overnight incubation at 37 °C, colony counts were determined, and the bacterial ratios of *S. aureus* and *S. lugdunensis* were calculated.

Co-colonization of cotton rat noses. For the colonization of cotton rat noses, spontaneous streptomycin-resistant mutants of *S. lugdunensis* IVK28 wild type and *S. lugdunensis* IVK28 Δ*lugD* were selected on BM agar plates containing 250 μg ml^{-1} streptomycin. Co-colonization was conducted with a streptomycin-resistant *S. aureus* Newman. The cotton rat model was described previously[43]. As the capacity of *S. lugdunensis* to colonize cotton rat nares has not been studied before, we determined the inoculum required for stable colonization by IVK28 wild type and its mutant Δ*lugD* over 5 days. Our previous studies have shown that for *S. aureus* an inoculum of 10^7 bacteria per nose results in a stable colonization of about 10^3 c.f.u. per nose (Extended Data Fig. 7a). To achieve a comparable colonization level with *S. lugdunensis*, an inoculum of 10^8 bacteria per nose was required, and there was no detectable difference in colonization efficiency between wild type and Δ*lugD* (Extended Data Fig. 7b, c). Therefore, co-colonization experiments in cotton rat noses were performed with tenfold more *S. lugdunensis* than *S. aureus* to obtain a 1:1 colonization ratio.

Cotton rats were anaesthetized and instilled intranasally with mixtures of either 1×10^8 *S. lugdunensis* wild type and 1×10^7 *S. aureus* Newman or 1×10^8 *S. lugdunensis* Δ*lugD* and 1×10^7 *S. aureus* Newman. Five days after bacterial instillation, the animals were euthanized, and noses were surgically removed. The noses were heavily vortexed in 1 ml of 1 × PBS for 30 s. Dilutions of the samples in PBS were plated on SSL agar containing 250 μg ml^{-1} streptomycin to select for the used strains and to separate *S. aureus* (yellow) and *S. lugdunensis* (purple) by colour. The plates were incubated for 2 days under anaerobic conditions (anaerobic jar with Anaerocult A, MerckKGaA), for the specific detection of ornithine decarboxylase activity. *S. aureus* Newman c.f.u. were determined afterwards. All animals received drinking water with 2.5 mg ml^{-1} streptomycin continuously, starting 3 days before the experiment, to reduce the natural nasal flora.

Human colonization study. A total of 187 nasal swab samples from hospitalized patients were received from the diagnostics laboratory of the Institute of Medical Microbiology and Hygiene (University Hospital Tübingen, Germany). Dilutions from each sample were plated on blood agar and SSL agar for a phenotypic identification of *S. aureus* and *S. lugdunensis*. Identity was confirmed by coagulase test and matrix-assisted laser desorption/ionization-time-of-flight mass spectrometry (mass spectrometer: AXIMA Assurance, Shimadzu Europa GmbH, Duisburg, database: SARAMIS with 23.980 spectra and 3.380 superspectra, BioMérieux, Nuertingen).

50. Ho, P. L. *et al.* Novel selective medium for isolation of *Staphylococcus lugdunensis* from wound specimens. *J. Clin. Microbiol.* **52,** 2633–2636 (2014).
51. Geiger, T. *et al.* The stringent response of *Staphylococcus aureus* and its impact on survival after phagocytosis through the induction of intracellular PSMs expression. *PLoS Pathog.* **8,** e1003016 (2012).
52. Winstel, V., Kühner, P., Krismer, B., Peschel, A. & Rohde, H. Transfer of plasmid DNA to clinical coagulase-negative staphylococcal pathogens by using a unique bacteriophage. *Appl. Environ. Microbiol.* **81,** 2481–2488 (2015).
53. Wenzel, M. *et al.* Small cationic antimicrobial peptides delocalize peripheral membrane proteins. *Proc. Natl Acad. Sci. USA* **111,** E1409–E1418 (2014).
54. Bandow, J. E., Brötz, H., Leichert, L. I., Labischinski, H. & Hecker, M. Proteomic approach to understanding antibiotic action. *Antimicrob. Agents Chemother.* **47,** 948–955 (2003).
55. Hutter, B. *et al.* Prediction of mechanisms of action of antibacterial compounds by gene expression profiling. *Antimicrob. Agents Chemother.* **48,** 2838–2844 (2004).
56. Sass, P. *et al.* Antibiotic acyldepsipeptides activate ClpP peptidase to degrade the cell division protein FtsZ. *Proc. Natl Acad. Sci. USA* **108,** 17474–17479 (2011).
57. Wang, R. *et al.* Identification of novel cytolytic peptides as key virulence determinants for community-associated MRSA. *Nat. Med.* **13,** 1510–1514 (2007).
58. Bara, R. *et al.* Atropisomeric dihydroanthracenones as inhibitors of multiresistant *Staphylococcus aureus*. *J. Med. Chem.* **56,** 3257–3272 (2013).
59. Wanke, I. *et al. Staphylococcus aureus* skin colonization is promoted by barrier disruption and leads to local inflammation. *Exp. Dermatol.* **22,** 153–155 (2013).

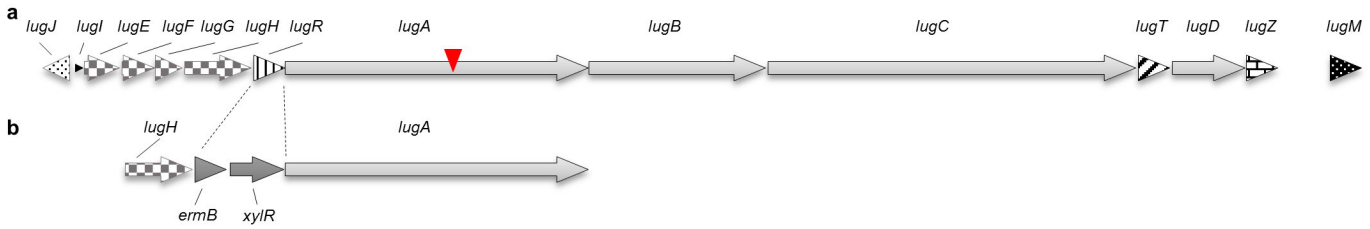

Extended Data Figure 1 | Gene cluster of lugdunin and generation of *S. lugdunensis* IVK28-Xyl. a, The lugdunin genes are located on a 30-kbp operon. *lugA–D* encode the four NRPS, which are preceded by the putative regulator gene *lugR*. Encoded upstream are putative ABC transporter genes (*lugE–H*) and genes for proteins with no described function (*lugI* and *lugJ*). A type-II thioesterase, that functions as a repair enzyme for stalled PCP domains, is encoded between *lugC* and *lugD*. The 4'-phosphopantetheinyl transferase LugZ converts inactive PCPs (apo-PCP) into the active holo-form by attachment of the 4'-phosphopantetheine cofactor. Encoded downstream is a putative monooxygenase (*lugM*). The transposon insertion site of Tn917, generating the lugdunin-deficient mutant IVK28 M1, is indicated by a red arrow. **b**, The xylose-inducible lugdunin producer strain *S. lugdunensis* IVK28-xyl was generated by replacement of the regulator gene *lugR* by the *xylAB* promoter along with the *xylR* gene encoding a xylose-sensitive repressor. The erythromycin resistance cassette *ermB* was integrated for selection purposes.

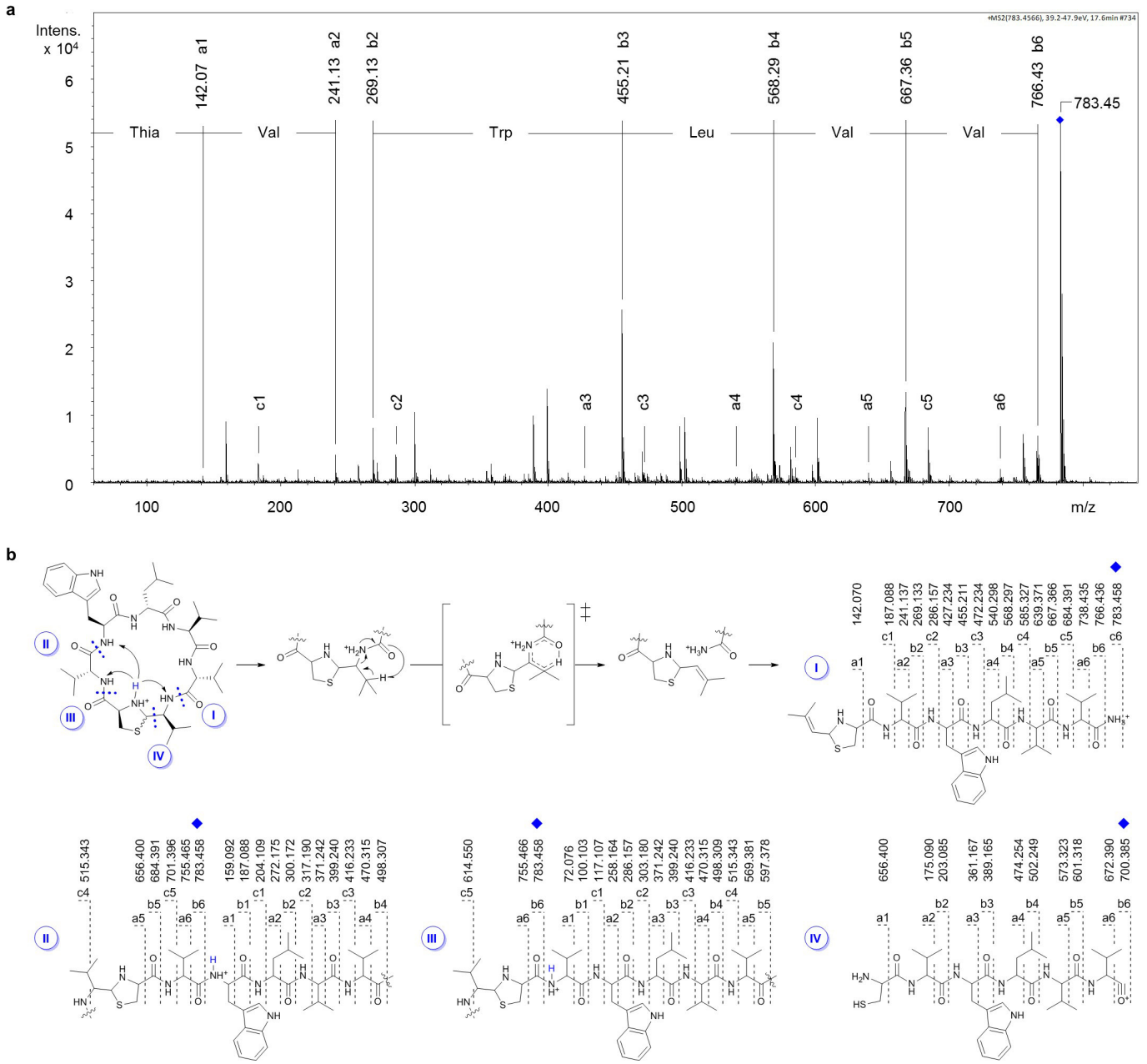

Extended Data Figure 2 | Structure elucidation by multistage tandem and electrospray ionization high-resolution mass spectrometry. **a**, A single-stage high-resolution MS/MS experiment revealed a superposition of fragment ions typically found for cyclic peptides. Quasi molecular ion selected for fragmentation is marked with a blue rhombus ($m/z = 783.45$). For sequence annotation, fragment ions were searched for b-ions of high intensity. One fragmentation route is annotated exemplarily by highlighting respective a-, b- and c-ion series signals. Thia, thiazoldine. **b**, Data generated by multistage tandem mass spectrometry show that lugdunin mainly fragmented along four routes (blue digits; (I), (II), (III), (IV)). Initial protonation occurs at the secondary amine of thiazolidine (blue H atom). Proton transfer to nearby peptide bonds initiated ring cleavage with subsequent fragmentation. Initial loss of ammonia for fragmentation route (I) can be explained by a precedent six-membered transition state. Intensities are in arbitrary units. Blue rhombuses label the position of initial ring cleavage. Fragmentation route molecules are shown in linearized form.

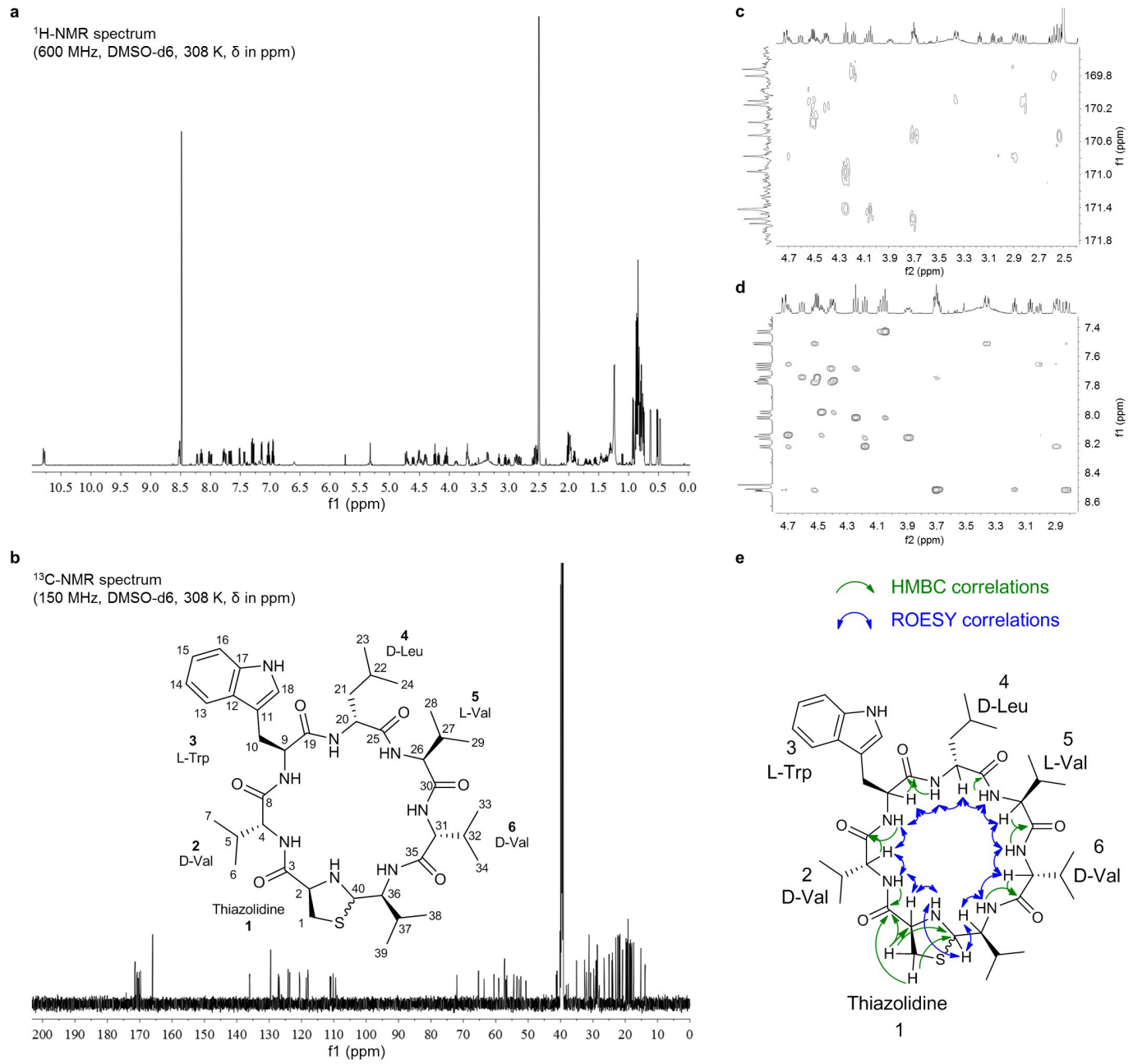

Extended Data Figure 3 | NMR spectra of the natural product lugdunin. The two diastereomeric and interconvertible forms of lugdunin (see imine intermediate, Extended Data Fig. 4d) show distinctive sets of NMR signals with consistent patterns, which were assigned by two-dimensional NMR methods (COSY, HMBC, HSQC-DEPT, ROESY and TOCSY) and corroborated the thiazolidine heterocycle as a special feature of lugdunin. Chemical shifts (δ) are shown in p.p.m. **a**, ^{1}H NMR spectrum (600 MHz) of lugdunin in DMSO-d6 at 308 K. **b**, ^{13}C NMR spectrum (150 MHz) of lugdunin in DMSO-d6 at 308 K. Atom numbering refers to full spectral assignment shown in Extended Data Table 1. **c**, Expansion of HMBC spectrum (heteronuclear multiple bond correlation) shows distinct correlations between the amino acid α-proton and the carbonyl C-atom of the respective amino acid. **d**, Expansion of ROESY spectrum (rotation frame nuclear Overhauser effect spectroscopy) shows short-ranged correlations through space between α-protons and amino acid amide protons. **e**, Taken together, HMBC (green arrows) and ROESY (double headed blue arrows) correlations allowed for a full sequential walk along the peptide backbone, which readily confirmed the amino acid sequence of both lugdunin diastereomers (the sequential walk is exemplarily shown for one diastereomer).

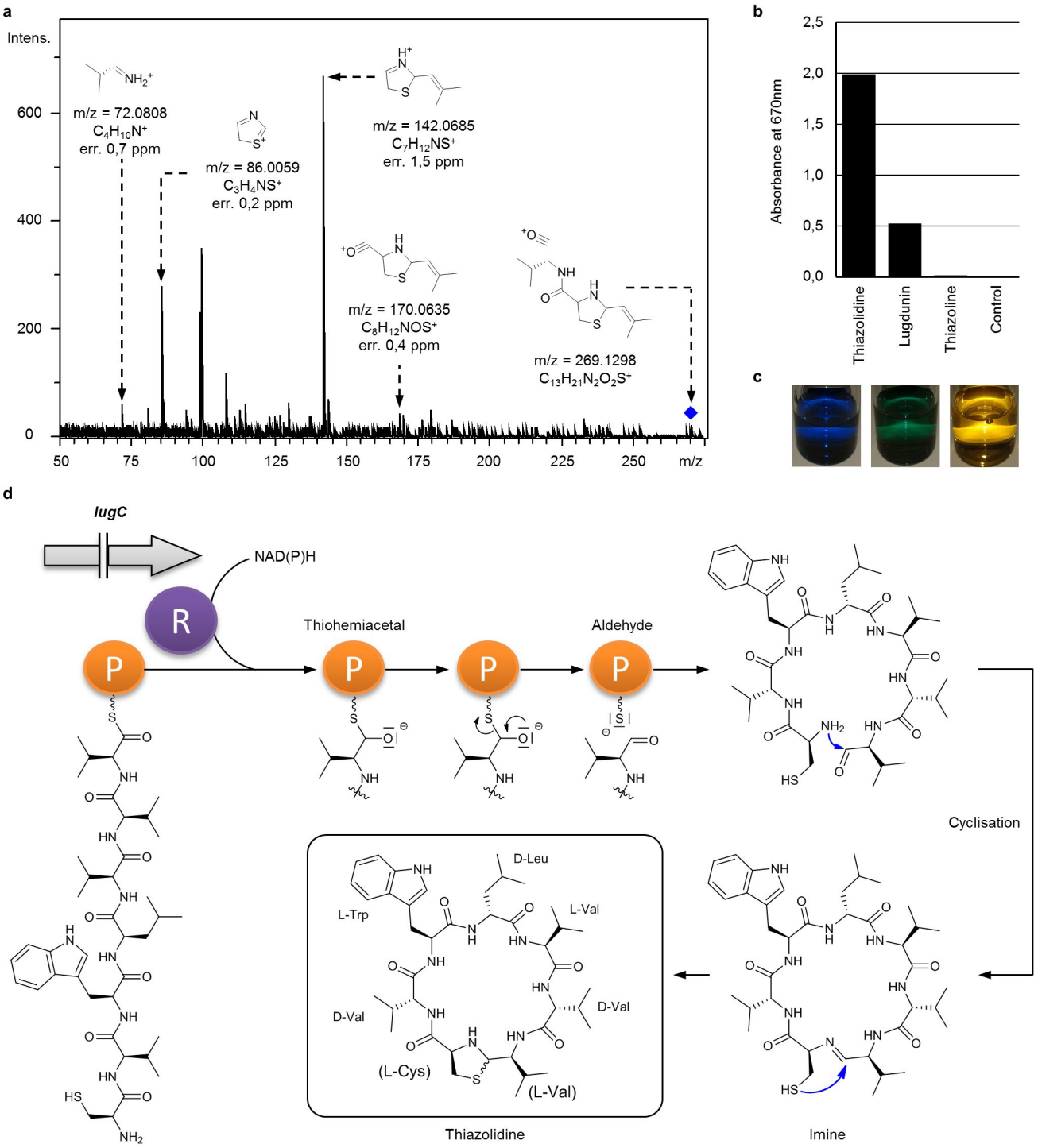

Extended Data Figure 4 | The thiazolidine moiety of lugdunin and its formation by peptide cyclisation. a, Blue rhombus marks the b2-ion from fragmentation route I (Extended Data Fig. 2). The ion was selected from an in-source collision-induced decay (isCID) experiment and was further fragmented in order to find thiazolidine-specific fragment ions. High-resolution MS data are shown with annotated sum formulas and respective deviations from calculated masses (errors in p.p.m.). Shown fragment ions reveal the b1-ion at $m/z = 170.0635$ Da. Intensity is shown in arbitrary units. **b**, Photometric detection of thiazolidines at 670 nm. A positive colour reaction with 3-methyl-2-benzothiazolone hydrazone hydrochloride (Sawicki reagent) gives rise to detectable absorbance at 670 nm. Thiazolidine-4-carboxylic acid (thiazolidine) was chosen as positive control, whereas 2-methyl-2-thiazoline (thiazoline) and DMSO acted as negative controls. **c**, Observable colours for the thiazolidine detection reaction. Thiazolidine-4-carboxlic acid (blue), lugdunin (green) and negative controls (yellow). **d**, The terminal reductase of LugC is proposed to initiate cleavage of the thioester-bound peptide chain with the aid of an NAD(P)H cofactor. The mature heptapeptide is liberated reductively from the NRPS multienzyme complex and cyclises via the N-terminal amine (L-Cys) and C-terminal aldehyde (L-Val) to form a macrocyclic imine/Schiff base. Subsequent nucleophilic attack of the cysteine thiol group generates the five-membered thiazolidine heterocycle. Nucleophilic attack by the L-cysteine sulfhydryl group may occur either at the *re* or *si* face of the imine thus leading to a diastereomeric mixture of two structural populations (depicted with wavy bond). *LugC* is shown as truncated gene, as indicated by the two lines (||).

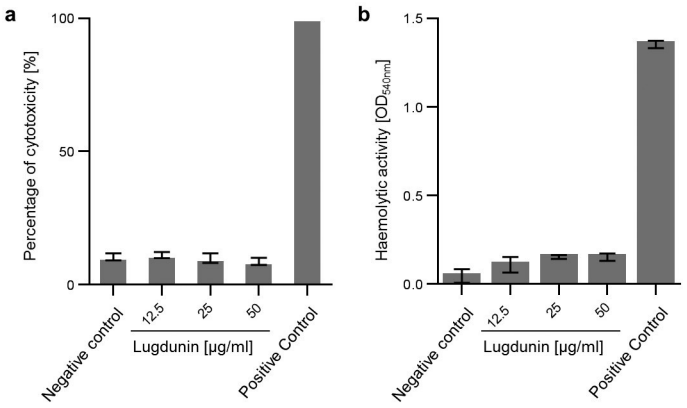

c

Compound	HL60 - promyelocytic leukemia cells IC_{50} [µg/ml]
Lugdunin	> 50
Staurosporine	2

IC_{50}, 50 % inhibitory concentration

Extended Data Figure 5 | Lugdunin activity against eukaryotic cells. **a**, **b**, Human neutrophil granulocytes (**a**) or erythrocytes (**b**) were incubated with high concentrations of lugdunin. Their lysis was monitored by the release of the enzyme lactate dehydrogenase (**a**) or haemoglobin (**b**), respectively. Cells without lugdunin were used as negative control. Incubation of cells in 2% Triton X-100 was used as positive control for high lysis. The data represent three independent experiments ± s.d. **c**, Promyelocytic leukaemia (HL60) cells were incubated with high concentrations of lugdunin. In order to determine the 50% inhibitory concentration of lugdunin, the metabolic activity of HL60 cells was measured by the conversion of resazurin into the highly fluorescent resorufin. The apoptosis-inducing staurosporine was used as positive control. IC_{50} values were calculated from the means of three independent experiments.

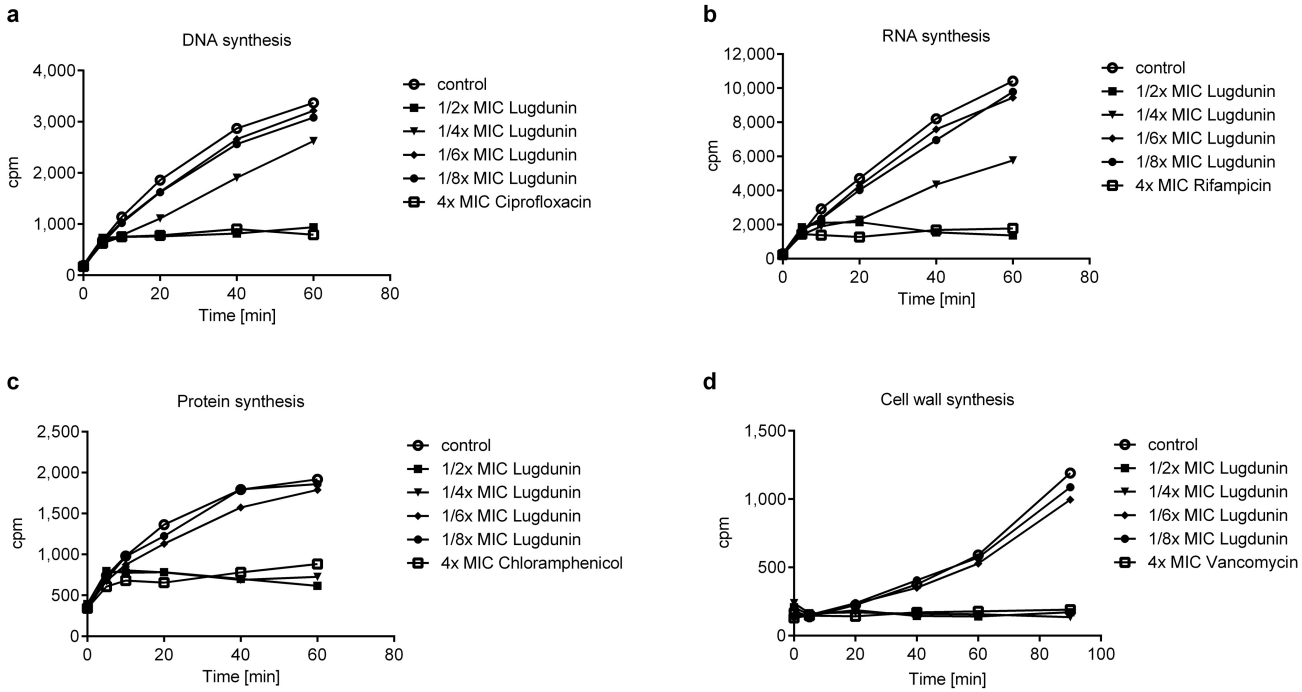

Extended Data Figure 6 | Time course of incorporation of tritium-labelled metabolic precursors into lugdunin-treated *B. subtilis*. *B. subtilis* 168 (trpC2) is a widely used model organism for mode of action investigations and was also used for orienting studies on the mechanism of lugdunin. Susceptibility of *B. subtilis* and *S. aureus* to lugdunin is similar (Table 1), with an MIC for *B. subtilis* of 4 $\mu g\,ml^{-1}$ in the Belitzky minimal medium used in this assay. **a**–**d**, Incorporation of thymidine into DNA (**a**), uridine into RNA (**b**), leucine into protein (**c**) or *N*-acetylglucosamine into peptidoglycan (**d**) ceased within minutes during lugdunin treatment. The experiment was repeated on three days with three independent bacterial cultures. One representative experiment is shown. At a concentration of half the MIC (1/2 MIC), incorporation of precursors into all pathways ceased reproducibly. At 1/8 MIC, incorporation continued repeatedly in parallel with the untreated control. At 1/4 MIC, the depicted experiment shows protein and peptidoglycan syntheses slightly more impaired than DNA and RNA syntheses, whereas the opposite occurred in another experiment. In summary, all four metabolic pathways seem to be equally impaired by lugdunin.

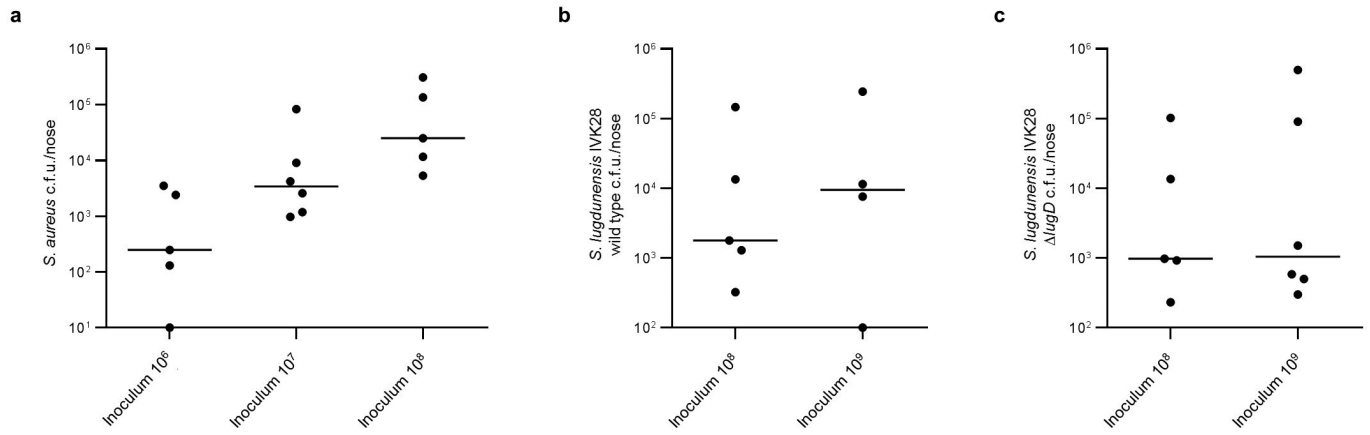

Extended Data Figure 7 | Nasal colonization rates by *S. aureus* and *S. lugdunensis* in cotton rats. a–c, Different inocula of *S. aureus* Newman (**a**), *S. lugdunensis* IVK 28 wild type (**b**) and *S. lugdunensis* IVK 28 Δ*lugD* (**c**) were instilled intranasally to determine their efficiency to colonize the noses of cotton rats (5 or 6 animals per group). c.f.u. of each strain were determined per nose after 5 days and plotted as individual dots. Lines represent the median of each group.

Extended Data Table 1 | NMR spectral assignment of lugdunin diastereomers

	Diastereomer I		Diastereomer II		
C-Atom	**δ_C**	**δ_H (mult., *J* in Hz)**	**δ_C**	**δ_H (mult., *J* in Hz)**	**C-Atom**
		1 L-Cys-Thiazolidine			
2-NH	-	2.88 (1H, m)	-	n.d.	2-NH
1	38.2	2.58 (1H, m) 3.06 (1H, dd, 9.7, 6.4)	37.5	2.54 (1H, m) 3.17 (1H, dd, 9.2, 6.0)	1
2	63.3	3.89 (1H, m)	65.3	3.69 (1H, m)	2
3	169.8	-	171.5	-	3
		2 D-Val			
4-NH	-	8.16 (1H, d, 9.8)	-	8.52 (1H, d, 8.6)	4-NH
4	57.2	4.18 (1H, dd, 10.0, 8.4)	60.5	3.70 (1H, m)	4
5		1.65 (1H, m)	28.5	1.71 (1H, m)	5
6, 7	18.6, 18.0	0.47 (3H, d, 6.6), 0.63 (3H, d, 6.6)	18.5, 19.3	0.52 (3H, d, 6.8), 0.84 (3H, m)*	6, 7
8	169.7	-	170.5	-	8
		3 L-Trp			
9-NH	-	8.22 (1H, d, 8.5)	-	8.52 (1H, d, 7.4)	9-NH
9	52.7	4.70 (1H, ddd, m)	53.4	4.52 (1H, m)	9
10	28.0	2.89 (1H, m) 3.01 (1H, dd, 14.0, 5.5)	26.4	2.82 (1H, dd, 14.7, 4), 3.36 (1H, dd, 14.7, 4)	10
11	109.5	-	110.2	-	11
12	127.1	-	126.8	-	12
13	118.2	7.66 (1H, d, 7.9)	117.9	7.51 (1H, d, 7.9)	13
14	117.9	6.95 (1H, ddd, 7.9, 7.8, 1.1)	118.1	6.96 (1H, ddd, 7.9, 7.9, 1.0)	14
15	120.5	7.02 (1H, ddd, 7.9, 7.8, 1.1)	120.7	7.04 (1H, ddd, 8.0, 7.9, 1.0)	15
16	110.9	7.28 (1H, dd, 7.9, 1.0)	111.1	7.30 (1H, dd, 8.0, 1.0)	16
17	136.0	-	136.1	-	17
18-NH	-	10.77 (1H, d, 2.0)	-	10.80 (1H, d. 2.0)	18-NH
18	124.1	7.15 (1H, d, 2.0)	123.6	7.15 (1H, d, 2.0)	18
19	170.8	-	170.1	-	19
		4 D-Leu			
20-NH	-	8.14 (1H, d, 8.7)		7.78 (1H, d, 9.4)	20-NH
20	50.7	4.46 (1H, ddm)	52.2	4.41 (1H, m)	20
21	41.3	1.32 (1H, m), 1.40 (1H, m)	41.1	1.30 (1H, m), 1.37 (1H, m)	21
22	24.1	1.28 (1H, m)	23.9	1.24 (1H, m)	22
23, 24	19.1, 19.3	0.84 (3H, m), 0.87 (3H, m)	20.8*, 21.6*	0.79 (3H, m), 0.77 (3H, m)	23, 24
25	171.6	-	171.4	-	25
		5 L-Val			
26-NH	-	7.99 (1H, d, 9.2)	-	7.69 (1H, d, 9.3)	26-NH
26	56.9	4.39 (1H, m)	57.4	4.24 (1H, dd, 9.2, 9.2)	26
27	31.2	1.96 (1H, m)	29.7	1.89 (1H, m)	27
28, 29	19.1, 17.9	0.80 (3H, m), 0.83 (3H, m)	19.1, 19.3	0.85 (3H, m)*, 0.84 (3H, m)*	28, 29
30	170.2	-	171.0	-	30
		6 D-Val			
31-NH	-	7.77 (1H, d, 8.7)	-	8.02 (1H, d, 7.8)	31-NH
31	56.5	4.50 (1H, dd, 8.8, 4.6)	59.1	4.04 (1H, dd, 7.8, 7.8)	31
32	31.9	1.97 (1H, m)	29.0	1.98 (1H, m)	32
33, 34	17.4, 19.1	0.83 (3H, d, 6.5), 0.88 (3H, d, 6.5)	18.3, 19.1	0.88 (3H, m), 0.84 (3H, m)	33, 34
35	170.4	-	171.4	-	35
		7 L-Val-Thiazolidine			
36-NH	-	7.74 (1H, d, 9.2)	-	7.43 (1H, d, 9.3)	36-NH
36	57.2	3.70 (1H, m)	54.4	4.04 (1H, dm, 9.3)	36
37	29.2	1.99 (1H, m)	32.5	1.55 (1H, m)	37
38, 39	15.2,22.3	0.75 (3H, d, 6.9), 0.79 (3H, d, 6.9)	19.8,19.7	0.86 (3H, d, 6.7), 0.92 (3H, d, 6.7)	38, 39
40	72.0	4.60 (1H, dd, 10.6, 8.8)	72.1	4.73 (1H, dd, 13.1, 2.0)	40

Chemical shifts (δ) are given in p.p.m. Mult., multiplicity. Coupling constants (*J*) are given in Hertz (Hz). Asterisks (*) mark strong signal overlap.

Extended Data Table 2 | Primers used in this study

Primer	Primer sequence 5'-3'	Gene annotation in *S. lugdunensis* N920143	Application for
Tn917 up	ATAGGCCTTGAAACATTGGTTTAGTGGG	---	Sequencing of transposon insertion site
Tn917 down	CCCATAGATAAGAAATACACCTGCAATAACC	---	Sequencing of transposon insertion site
SlPr1-up	TACGGTACCCGCTTAACAAGATGACTAGC	SLUG_RS03935	Replacement of *lugR* by *xylAP* promoter and *xylR* regulator gene
SlPr1-down	TCTTTATGGTACCTATTACATCTCTAAAG	SLUG_ RS03935	Replacement of *lugR* by *xylAP* promoter and *xylR* regulator gene
SlPr2-up	ATTTGTATTGATATCATAAAAAATGTCCG	SLUG_ RS03935	Replacement of *lugR* by *xylAP* promoter and *xylR* regulator gene
SlPr2-down	GTTAGATCTAAAGGAGGTCAATCAGATGG	SLUG_ RS03935	Replacement of *lugR* by *xylAP* promoter and *xylR* regulator gene
lugD upstream-SacI	TAGGAGCTCGCTTAATGAATTC	SLUG_RS03965	*S. lugdunensis* Δ*lugD*
lugD upstream-Acc65I	ATAGGTACCCTCCTTCTAGCTAAGC	SLUG_RS03965	*S. lugdunensis* Δ*lugD*
lugD downstream-Acc65I	AGTGGTACCCTCTATTAACTGAAAGG	SLUG_RS03965	*S. lugdunensis* Δ*lugD*
lugD downstream-BglII	ATTAGATCTGAAGTTAAGCATCCGTC	SLUG_RS03965	*S. lugdunensis* Δ*lugD*
lugD comp. forw-PstI	ATACTGCAGGCTTAGCTAGAAGGAGAG	SLUG_RS03965	Complementation of *S. lugdunensis* Δ*lugD*
lugD comp. rev-Acc65I	AATGGTACCCATCAGCATTATAGTT	SLUG_RS03965	Complementation of *S. lugdunensis* Δ*lugD*

CORRIGENDUM

doi:10.1038/nature19781

Corrigendum: Human commensals producing a novel antibiotic impair pathogen colonization

Alexander Zipperer, Martin C. Konnerth, Claudia Laux, Anne Berscheid, Daniela Janek, Christopher Weidenmaier, Marc Burian, Nadine A. Schilling, Christoph Slavetinsky, Matthias Marschal, Matthias Willmann, Hubert Kalbacher, Birgit Schittek, Heike Brötz-Oesterhelt, Stephanie Grond, Andreas Peschel & Bernhard Krismer

Nature **535,** 511–516 (2016); doi:10.1038/nature18634

In the interests of transparency, in this Article we wish to amend the competing financial interests statement to read: "Tuebingen University has filed a provisional patent application that covers the compound lugdunin and derivatives thereof, as well as the application of lugdunin-producing bacteria for the prevention of bacterial infections (European patent application number EP 15 160 285.1)." The online versions of the paper have been corrected.